Article

Forecasting Streamflow under Combined Climate and Land-Use/Cover Change Scenarios

Babak Farjad [1]*, Anil Gupta [2] and Danielle Marceau [3]

[1,3] Department of Geomatics Engineering, University of Calgary, 2500 University Drive NW, Calgary, AB, Canada T2N 1N4; [1] bfarjad@ucalgary.ca; [3]dmarceau@ucalgary.ca
[2] Alberta Environment and Parks, Calgary, AB, Canada AB T3L 1S4; anil.gupta@gov.ab.ca
* Correspondence: bfarjad@ucalgary.ca; Tel.: ++1-403-220-8794

Abstract: This study was undertaken to investigate the responses of streamflow to the combined impact of climate and LULC change in the watershed in the 2020s and 2050s. The physically-based, distributed MIKE SHE/MIKE 11 model was coupled with a LULC cellular automata model to simulate streamflow using two extreme GCM-scenarios and two LULC change scenarios. Results reveal that LULC change is the dominant factor affecting the majority of the hydrological processes, especially streamflow, and that it plays a key role in amplifying a rise in flow discharge in the Elbow River. The separated impacts of climate and LULC change on streamflow are positively correlated in winter and spring, which intensifies their influence. This is particularly the case in spring when the combined impact of climate and LULC results in a significant rise in streamflow, which may increase the vulnerability of the watershed to floods in this season. This study clearly reveals that climate and land-use/cover change will induce significant modifications on either the annual or the seasonal streamflow in the watershed.

Keywords: Climate change; land-use change; Streamflow; Hydrological processes; Water resources management

PACS: J0101

1. Introduction

In the future, water stress is predicted to increase across the world as a result of population growth and environmental and climate change [1, 2]. Around five billion people (out of a world population of around eight billion people) are expected to live in areas that are vulnerable to fluctuations in water supply and water stress by 2025 [3]. Climate change and land-use/land-cover (LULC) change are two main factors that can directly alter water supply [4]. For instance, changes in LULC can modify the total annual runoff [5], streamflow, while changes in climate are associated with extreme events frequency [6].

Numerous studies have been conducted to investigate hydrological responses to climate change. They focused on the responses of hydrological processes to climate change [7, 8, 9, 10, 11], while neglecting to account for changes in LULC over time. Other studies have focused on the changes in hydrological processes due to changes in LULC [12, 13, 14]; however they assumed the climate variables were constant. Addressing the limitations of the previous studies, this research aims at understanding the relationship between climate, LULC, and hydrology using an integrated modeling framework which consists of three major components: (i) a LULC change cellular automata (CA) model, (ii) the distributed physically-based, MIKE SHE/MIKE 11 model, and (iii) GCM-scenarios. The framework is applied to the Elbow River watershed in southern Alberta, Canada to understand how streamflow responds to both LULC and climate change.

1.2. The Elbow River watershed

The Elbow River watershed, located in southern Alberta, drains approximately 1235 km^2. The Elbow River originates at Elbow Lake and flows 120 kilometers long through the alpine, subalpine, boreal foothill, and aspen parkland before joining the Bow River in downtown Calgary. The river supplies the Glenmore Reservoir that provides water to nearly half of the City of Calgary, and water uses such as industrial and irrigation for agriculture. In terms of LULC, the watershed is comprised of urban areas (5.9%), agriculture (16.7%), rangeland/parkland (6.2%), evergreen forest (34%), deciduous forest (10%), and clear-cuts (1.8%) (Figure 1).

Models of future climate trends along with population growth scenarios have indicated that Calgary will face significant water supply challenges in the future. For this city to maintain a sustainable water supply, it will require water conservation efforts to reduce the per-capita water consumption to less than 50% of the current level by 2064. Even then, in the hot and dry projected periods, water demand could exceed the supply allotments [15]. As a result, the Province of Alberta has stopped accepting new applications for the allocation of water since August 2006 in the Bow River basin (the Elbow River is an important multi-use tributary of the Bow River Basin) [16].

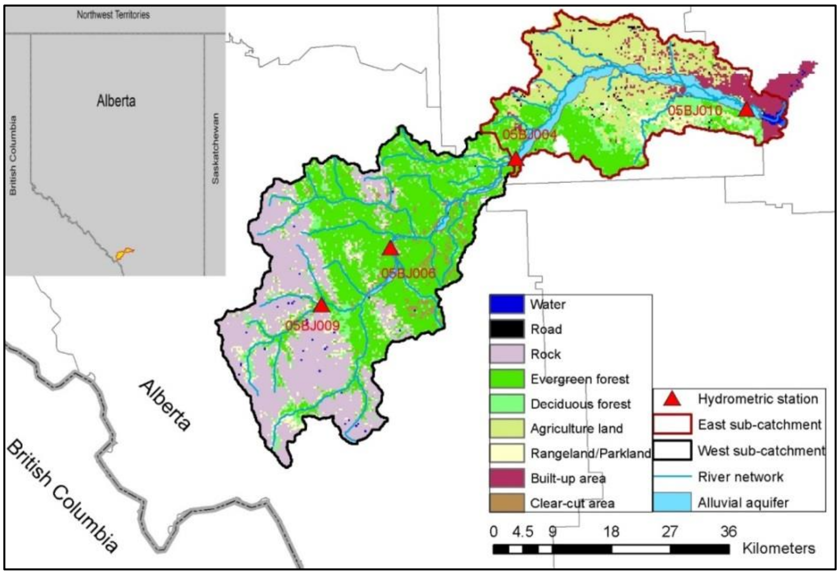

Figure 1. Location of the Elbow River watershed

2. Method

2.1. Land-use/land-cover modelling

A cellular automata (CA) model was developed to project future LULC changes in the study area. CA is a rigorous modeling approach for characterizing complex spatial systems through a bottom up simulation of local interactions between neighboring cells. A typical CA consists of five main elements [17]: 1) geographic space that is represented by a grid of cells, 2) cell states that define the set of possible values associated to the cells, 3) a neighborhood of adjacent cells that can influence the central cell, 4) transition rules that define the next state of the central cells according to their states, the states of the adjacent cells in the neighborhood, and some external factors, and 5) time step which is discrete for all cells to change state simultaneously.

The LULC maps of 1985, 1992, 1996, 2001 and 2006 were used to calibrate the CA model. A sensitivity analysis was conducted to evaluate the sensitivity of the simulation outcomes to the cell size, neighborhood configuration, external driving factor, and the method for selecting the ranges of values from frequency histograms. This analysis revealed that a cell size of 60 m, a three-ring neighborhood with a radius of 5, 9 and 17 cells (300, 540 and 900 m respectively), and all external driving factors where the most appropriate to obtain the best simulation outcomes. The considered driving factors (important factors that influence land-use changes) include distance to Calgary city center, distance to a main road, distance to a main river, and the ground slope. The model was validated by comparison of the simulated maps of 2006 and 2010 with the historical data using various metrics. Two opposite scenarios of LULC change, Lu-(PL) and Lu-(PH), which respectively represent lower and higher growth in economy, immigration, and population were identified to cover a plausible range of change in the study area. The LULC changes were simulated up to 2070 at a 10-year interval.

2.2. Hydrological modelling

The MIKE SHE/MIKE 11 model was used to simulate streamflow in the 2020s and 2050s. MIKE SHE/MIKE 11 is a distributed physically based modeling system capable of simulating the entire processes occurring in the land phase of the hydrologic cycle. MIKE SHE includes a full suite of pre- and post-processing tools and advanced solution techniques for hydrological components such as overland flow, unsaturated flow, and saturated flow, and their interactions. MIKE 11 is a fully dynamic and one-dimensional hydraulic model that simulates flows, rivers, channels, and other water bodies. MIKE SHE and MIKE 11 are coupled to address the interactions between stream flow and groundwater.

In this research, MIKE SHE was used to estimate overland flow using a finite difference method to solve a two-dimensional diffusive wave approximation of the Saint Venant equations.

$$\boldsymbol{u}h = K_x \times [\![(-\partial z/\partial x)]\!]^{\wedge(1/2)} \times h^{5/3} \quad (1)$$

$$\boldsymbol{v}h = K_y \times [\![(-\partial z/\partial y)]\!]^{\wedge(1/2)} \times h^{5/3} \quad (2)$$

where h (m) is the water level on the ground surface, $\boldsymbol{u}h$ and $\boldsymbol{v}h$ (m^2s^{-1}) are discharge, K_x and K_y are Manning M in the x and y directions. The equation for the flow between grid cells is:

$$Q = K\Delta x/[\![\Delta x]\!]^{(1/2)} \ (Z_u - Z_D)^{1/2} h_u^{5/3} \quad (3)$$

where Z_u and Z_D (mm) are the maximum and minimum water levels.

The equations for the MIKE 11 are the vertical integration of conservation of volume and momentum.

$$(\partial Q/\partial x)+(\delta A/\delta t)=q \quad (4)$$

$$(\delta Q/\delta t)+\delta[(\alpha Q^2/A)/\delta x]+[gA\,(\delta h/\delta x)]+[(gQ|Q|)/(C^2 AR)]=0 \quad (5)$$

where Q is the discharge, A is the flow, q is the lateral inflow, h is the stage above datum, C is the Chezy resistance coefficient, R is the hydraulic or resistance radius, and α is the momentum distribution coefficient. In order to model groundwater, a 3D finite difference method was used based on the 3-dimensional Darcy equation.

$$\partial/\partial x\,[k_h\,(\partial h/\partial x)]+\partial/\partial y\,[k_h\,(\partial h/\partial y)]+\partial/\partial z\,[k_v\,(\partial h/\partial z)]-Q=S(\partial h/\partial t) \quad (6)$$

where h(x,y,z) is the hydraulic head, K_v and K_h are the vertical and horizontal hydraulic conductivity. S is the specific storage coefficient, and Q is the volumetric source.

A sensitivity analysis was conducted to select the most suitable parameters for the MIKE SHE/MIKE 11 in the watershed. The model was also calibrated and validated using three methods [7]. The first one was the split-sample method that emphasizes different time intervals for calibration and validation while a different land-use map was used for validation in each time interval. The second one was the multi-criteria method that uses different criteria to evaluate the goodness of fit based on different types of data. The third one was the multi-point method that applies different locations of observed data for calibration from the location which were selected for validation.

The calibration of the model was carried out for the period of 1981-1991 with a LULC map of 1985. Four time periods (1991-1995, 1995-2000, 2000-2005, and 2005-2008) were used for validation with their corresponding LULC maps (1992, 1996, 2001, and 2006). The goodness-of-fit was evaluated by comparing observed data and simulated data of total snow storage, stream flow, and groundwater levels.

2.3. Climate change scenarios

The output of two climate models: the CGCM2 (Canadian Centre for Climate Modelling and Analysis) and the NCARPCM (National Centre for Atmospheric Research), forced by two climate scenarios: A1B [18] and B2 [19], were used to construct time series climate variables for the periods of 2020s (2011-2040) and 2050s (2041-2070). The A1B scenario assumes a world of very rapid global economic and population growth with peaks in mid-century, whereas B2 describes lower growth rates of the global economic and population.

The climate variables associated with these scenarios include temperature and precipitation over two periods (2020s and 2050s) relative to 1961–1990. The widely used delta change method was utilized for downscaling climate model outputs into hydrological model inputs [10, 11, 20]. This method is easy to employ, but it has the limitation of retaining the temporal structure of the baseline data. To overcome this limitation, only changes in annual and seasonal responses of hydrological processes to climate scenarios were taken into account in this study [21].

2.4. Simulated scenarios

In order to investigate changes in streamflow, a base case scenario (BL) was defined to represent the baseline climate from 1961 to 1990 with the LULC map of 1985. Then, streamflow was simulated for the following scenarios over different time periods:

1) Impact of LULC change on streamflow:

a) LU-H scenario: this scenario assumes constant baseline climate (1961-1990) while LULC changes for the 2020s and 2050s under the Lu-(PH) scenario.

b) LU-L scenario: this scenario assumes constant baseline climate (1961-1990) while LULC changes for the 2020s and 2050s under the Lu-(PL) scenario.

2) Impact of climate change on streamflow:

a) A1B scenario: this scenario considers the A1B climate scenario while LULC is constant.

b) B2(3) scenario: this scenario considers the B2(3) climate scenario while LULC is constant.

3) Impact of climate and LULC change on streamflow:

a) LU(H)-A1B scenario: this scenario considers the A1B climate scenario with the LU- PH scenario.

b) LU(L)-A1B scenario: this scenario considers the A1B climate scenario with the LU- PL scenario.

c) LU(H)-B23 scenario: this scenario considers the B2(3) climate scenario with the LU- PH scenario.

d) LU(L)-B23 scenario: this scenario considers the B2(3) climate scenario with the LU- PL scenario.

3. Results and Discussion

The LULC change scenarios result in an increase in streamflow in the 2020s (8.1% and 7.5%) and 2050s (13.7% and 12.7%). Changes in streamflow under the A1B climate scenario occur in the same direction as with the LULC scenarios, which result in an increase in streamflow under the LU(H)-A1B and LU(L)-A1B scenarios in the 2020s and 2050s. On the other hand, LULC scenarios compensate the decline in streamflow under the B2(3) scenarios in the 2020s and 2050s.

The average seasonal streamflow increases under the combined and individual climate and LULC change scenarios in the winter and spring of the 2020s and 2050s. During these seasons, streamflow is strongly attributed to snowmelt, which in turn is more controlled by variations in temperature than precipitation. At high elevations in the watershed, precipitation falls predominantly as snow in the winter and accumulates in storage until spring melt, although snowmelt occurs in winter especially at low elevations when temperatures are above freezing, which results in a low flow through winter and early spring. In 2020s, winter streamflow increases under the A1B and B2(3) climate change scenarios by 5.9% and 2.5%, respectively, while it also increases under the LULC change scenarios by 3.4%. The direction of the change in streamflow affected by LULC change-alone and climate change-alone is the same; therefore, the rise in streamflow is enhanced in response to the combined climate and LULC scenarios. In the 2050s, the magnitude of change in winter streamflow under the A1B scenario (24.6%) is considerably larger than under the B2(3) scenario (1.6%); this can be associated with a rise in precipitation. This results in greater streamflow under the combined climate and LULC change scenarios, LU(H)-A1B and LU(L)-A1B, compared to the LU(H)-B23 and LU(L)-B23 scenarios. On the other hand, streamflow increases by 3.8-4% under the LULC scenarios, which is not a considerable change compared to A1B (24.6%); however it is greater than the increase under the B2(3) scenario (1.6%).

In spring, streamflow exhibits the largest variations in both the 2020s and 2050s. The greatest changes in spring occur under the LU(H)-A1B and LU(L)-A1B scenarios in the 2020s (28.3-29.4%) and 2050s (58.2-59.8%), respectively. This is mostly associated with the A1B climate scenario, which is the dominant driver compared to the LULC change scenarios and the B2(3) climate scenario. Streamflow increases considerably in the late spring for both climate scenarios due to a considerable rise in precipitation along with an intensified snowmelt. High flows can be even further amplified especially in the late spring when an increase in temperature can lead to a rise in a number of rain-on-snow events and eventually enhance the risk of flooding. Although there is a decline in precipitation under the B2(3) scenario in the 2020s, streamflow exhibits a increase in this season, which implies an intensified snowmelt.

In the summer, the climate change scenarios generate a decline in streamflow in the 2020s and 2050s, except with the A1B scenario in the 2050s when a slight increase can be observed. On the other hand, LULC change results in an increase in summer streamflow. Increasing streamflow in many watersheds has been attributed to LULC change [22, 23]. A change in LULC due to urbanization and deforestation can result in a decline in rainfall interception loss, canopy evapotranspiration, and a rise in converted units of rainfall to runoff and snowpack water equivalent. These changes are more pronounced in the summer when streamflow tends to respond directly and quickly to the precipitation that falls on the ground, mainly as rain. Simulation of summer streamflow indicates a rise under the LULC change scenarios, LU-H (8.1%) and LU-L (7.4%), in the 2020s. A rise in streamflow under the LU-H (8.1%) and LU-L (7.4%) scenarios creates a buffering effect on declining streamflow under the A1B (-5%) climate scenario, and eventually results in an increased streamflow under the LU(H)-A1B (2.4%) and LU(L)-A1B (1.8%) scenarios. However, the rise in streamflow affected by the LULC change scenarios cannot offset the decline in streamflow affected by the B2(3) (-11.8%) climate scenario, which results in a decrease in streamflow under the combined LU(L)-B2(3) (-4.1%) and LU(H)-B3(3) (-4.7%), scenarios. In the 2050s, the direction of changes in streamflow in the summer is the same as the 2020s, but with a higher magnitude, except for the A1B climate scenario, which causes a rise (3.7%) in streamflow in the 2050s and enhances the increase in LU(H)-A1B (19.9%) and LU(L)-A1B (18.8%).

In the fall, an increase in temperature can result in more water losses by evapotranspiration from the watershed, rather than a rise in the snowmelt when snowpack reaches a lower volume. Simulation shows that an increase in streamflow due to the LULC change scenarios and the A1B climate change scenario amplifies the rise in streamflow under the combined LU(H)-A1B (14.3–

25.4%) and LU(L)-A1B (13.9–24.7%) scenarios in the 2020s and 2050s, respectively. However, the B2(3) scenario compensates the LULC change impact and results in a small rise in streamflow in the LU(H)-B23 and LU(L)-B23 scenarios.

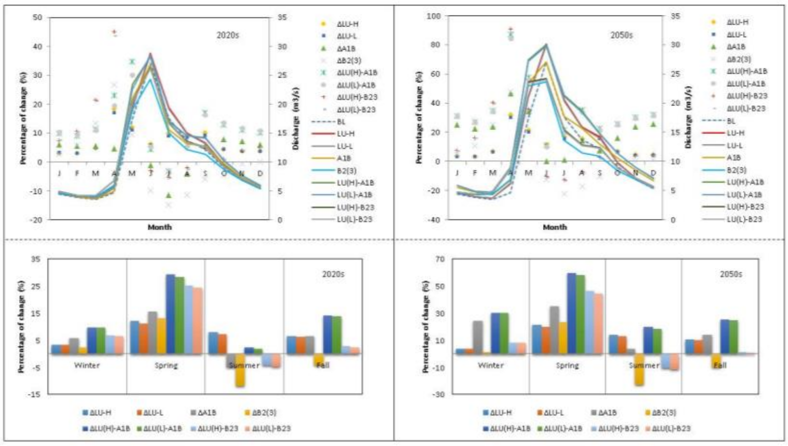

Figure 2. *Average seasonal changes in streamflow for the period of 2020s and 2050s relative to the baseline (1961-1990)*

4. Conclusion

This research describes the streamflow responses of the watershed under two extreme climate and LULC scenarios over the next 60 years using an integrated modeling system that incorporates the major components of climate, LULC, and hydrology. Results reveal that the LULC change scenarios result in an increase in the average annual streamflow, which amplifies the magnitude of rise associated with the A1B climate scenario and compensates for the decline linked to the B2(3) climate scenario. The largest rise in streamflow occurs in spring under both the climate and LULC scenarios. The separated impacts of climate and LULC change on streamflow are positively correlated in winter and spring, which intensifies their combined influence and may also increase the vulnerability of the watershed to floods in spring. Our findings highlight the fact that investigating the hydrological responses to climate change-alone or LULC change-alone may lead to an underestimation or overestimation of the hydrological response of a watershed.

Acknowledgments: This project was funded by a research grant awarded to Dr. Danielle Marceau by Tecterra and Alberta Environment and Parks, and by an Alberta Innovates Technology Futures graduate student scholarship awarded to Babak Farjad. We thank Patrick Delaney and Ying Qiao from DHI Water and Environment Canada for their insightful support..

Conflicts of Interest: The authors declare no conflict of interest.

References

1. Henderson-Sellers, A., Irannejad, P., & McGuffie, K. (2008). Future desertification and climate change: the need for land-surface system evaluation improvement. Global and Planetary Change, 64(3), 129-138.
2. Beck, L., & Bernauer, T. (2011). How will combined changes in water demand and climate affect water availability in the Zambezi river basin?. Global Environmental Change, 21(3), 1061-1072.
3. Arnell, N. W. (1999). Climate change and global water resources. Global environmental change, 9, S31-S49.
4. Gathenya, M., Mwangi, H., Coe, R., & Sang, J. (2011). Climate-and land use-induced risks to watershed services in the Nyando River Basin, Kenya. Experimental Agriculture, 47(02), 339-356.
5. He, M., & Hogue, T. S. (2012). Integrating hydrologic modeling and land use projections for evaluation of hydrologic response and regional water supply impacts in semi-arid environments. Environmental Earth Sciences, 65(6), 1671-1685.

6. Gathenya, M., Mwangi, H., Coe, R., & Sang, J. (2011). Climate-and land use-induced risks to watershed services in the Nyando River Basin, Kenya. Experimental Agriculture, 47(2), 339-356.
7. Farjad, B., Gupta, A., & Marceau, D. J. (2016). Annual and Seasonal Variations of Hydrological Processes Under Climate Change Scenarios in Two Sub-Catchments of a Complex Watershed. Water Resources Management, 30(8), 2851-2865.
8. Farjad, B., Gupta, A., & Marceau, D. J. (2015). Hydrological regime responses to climate change for the 2020s and 2050s periods in the Elbow River watershed in southern Alberta, Canada. In Environmental Management of River Basin Ecosystems (pp. 65-89). Springer International Publishing.
9. Hosseinizadeh, A., SeyedKaboli, H., Zareie, H., Akhondali, A., & Farjad, B. (2015). Impact of climate change on the severity, duration, and frequency of drought in a semi-arid agricultural basin. Geoenvironmental Disasters, 2(1), 1.
10. Kienzle, S. W., Nemeth, M. W., Byrne, J. M., & MacDonald, R. J. (2012). Simulating the hydrological impacts of climate change in the upper North Saskatchewan River basin, Alberta, Canada. Journal of Hydrology, 412, 76-89.
11. Forbes, K. A., Kienzle, S. W., Coburn, C. A., Byrne, J. M., & Rasmussen, J. (2011). Simulating the hydrological response to predicted climate change on a watershed in southern Alberta, Canada. Climatic change, 105(3-4), 555-576.
12. Wijesekara, G. N., Farjad, B., Gupta, A., Qiao, Y., Delaney, P., & Marceau, D. J. (2014). A comprehensive land-use/hydrological modeling system for scenario simulations in the Elbow River watershed, Alberta, Canada.Environmental management, 53(2), 357-381.
13. Thanapakpawin, P., Richey, J., Thomas, D., Rodda, S., Campbell, B., & Logsdon, M. (2007). Effects of landuse change on the hydrologic regime of the Mae Chaem river basin, NW Thailand. Journal of Hydrology, 334(1), 215-230.
14. Chu, H. J., Lin, Y. P., Huang, C. W., Hsu, C. Y., & Chen, H. Y. (2010). Modelling the hydrologic effects of dynamic land-use change using a distributed hydrologic model and a spatial land-use allocation model. Hydrological Processes, 24(18), 2538-2554.
15. Chen, Z., Grasby, S. E., Osadetz, K. G., & Fesko, P. (2006). Historical climate and stream flow trends and future water demand analysis in the Calgary region, Canada. Water science and technology, 53(10), 1-12.
16. Pernitsky, D. J., & Guy, N. D. (2010). Closing the South Saskatchewan River Basin to New Water Licences: Effects on Municipal Water Supplies. Canadian Water Resources Journal, 35(1), 79-92.
17. Moreno, N., Wang, F., & Marceau, D. J. (2009). Implementation of a dynamic neighborhood in a land-use vector-based cellular automata model. Computers, Environment and Urban Systems, 33(1), 44-54.
18. Zhang S, Gao X, Zhang X, Hagemann S (2012) Projection of glacier runoff in Yarkant River basin and Beida River basin, Western China. Hydrological Processes 26(18): 2773–2781.
19. Boyer, C., Chaumont, D., Chartier, I., & Roy, A. G. (2010). Impact of climate change on the hydrology of St. Lawrence tributaries. Journal of Hydrology, 384(1), 65-83.
20. Hay L E, McCabe G J (2010) Hydrologic effects of climate change in the Yukon River Basin. Climatic change 100(3-4): 509-523.
21. Köplin N, Schädler B, Viviroli D, Weingartner R (2013) The importance of glacier and forest change in hydrological climate-impact studies. Hydrology and Earth System Sciences 17(2): 619–635.
22. Costa M H, Botta A, Cardille J A (2003) Effects of large-scale changes in land cover on the discharge of the Tocantins River, Southeastern Amazonia. Journal of Hydrology 283(1): 206–217.
23. Peña-Arancibia J L, van Dijk A I, Guerschman J P, Mulligan M, Bruijnzeel L A, McVicar T R (2012) Detecting changes in streamflow after partial woodland clearing in two large catchments in the seasonal tropics. Journal of Hydrology 416: 60–71